

STUDY ON CRYSTAL STRUCTURE AND MAGNETIC PROPERTIES OF $Ba_4Co_2Fe_{36}O_{60}$ BY SOL-GEL METHOD

U-type ferrite typified by $Ba_4Co_2Fe_{36}O_{60}$ is used as a RAM (Radar Absorbing Materials) in the X-band (8-12 GHz). $Ba_4Co_2Fe_{36}O_{60}$ is known to have a complex crystal structure, which makes it difficult to obtain single phase and have low reproducibility. Previously known U-type ferrites have been fabricated based on a ceramic process that mixing (by a ball mill), calcining, grinding, binder mixing, drying, sieving, pressing and sintering. In contrast, the process of preparing the powder by the sol-gel method and its heat-treating is advantageous in that it can reduce the process steps and the required time. In addition, the precise stoichiometric control by the sol-gel method can effectively evaluate the effect of added or substituted elements. In this study investigates the crystal structure of $Ba_4Co_2Fe_{36}O_{60}$ synthesized by the sol-gel method and the morphology of U-type ferrite nano-powders according to various heat treatment conditions. Analysis of the crystal structure is used for XRD. Morphology and size are observed by SEM. In addition, VSM is performed to confirm the change of magnetic properties according to various heat treatment conditions.

Keywords: U-type ferrite, Sol-gel method, Nano-powder

1. Introduction

Ferrite is the most commonly known microwave absorber and various types of ferrite are widely used [1,2]. Among them, hexagonal ferrite (hexaferrite) materials are high interest in the last decade from materials that can be used as a microwave absorber in the GHz frequency range [1-3]. There are various phases of M, Y, W, Z, X and U-type in hexaferrite, and U-type hexaferrite has been continuously studied in radar absorbing materials especially in X-band (8-12 GHz) region [1-4].

U-type ferrite has a complex crystal structure and a large unit cell [1, 2], and its general formula is represented by $A_4B_2Fe_{36}O_{60}$ where A is Ba or Sr and B is divalent transition metal ion (Mn, Fe, Co, Ni, Zn, etc.). The study on the conventional U-type ferrite is classified into two kinds of flow. One flow is focused on the absorption characteristics change depending on the influence of the element substituted in the A or B site [2]. The effect of the substituted element appears as a phenomenon such as a change in absorption frequency range or a difference in absorption rate. The other is to identify the cause of the difference in the absorption characteristics through various analysis methods [5-7]. However, in comparison with various studies on the effect of substitutional elements, there is a relatively insufficient study on the characteristic difference according to the fabrication method of the U-type ferrite.

Most of the conventional U-type ferrite has fabricated by a ceramic process (or solid state reaction process) [8-12]. In

this study, U-type ferrite has synthesized based on the previous research on ferrite fabrication by sol-gel method [13,14] and then heat treated to fabricate nano-powder. To investigate the change in the heat treatment condition of the nano-powder has analyzed crystal structure and magnetic properties. We have investigated the possibility of fabricating U-type ferrite by sol-gel method and the difference of crystal structure, grain size and morphology and magnetic properties between the U-type ferrite by sol-gel method and the conventional U-type ferrite. In addition, it will be used as a reference for future studies.

2. Experimental

In this study, $Ba_4Co_2Fe_{36}O_{60}$ U-type ferrite was prepared by sol-gel method. Barium nitrate ($Ba(NO_3)_2$, 98.5%, DAEJUNG CHEMICALS & METALS), cobalt acetate tetrahydrate ($(CH_3COO)_2Co \cdot 4H_2O$, 98.0%, DAEJUNG CHEMICALS & METALS), iron nitrate nonahydrate ($Fe(NO_3)_3 \cdot 9H_2O$, 98.5%, SAMCHUN CHEMICAL) were used as starting raw materials and mixed in deionized water by the stoichiometric ratio. Citric acid ($C_6H_8O_7$, 99.0%, Alfa Aesar) and ethylene glycol ($C_2H_6O_2$, 98.5%, DAEJUNG CHEMICALS & METALS) was added to the mixture. And then, the mixture had adjusted to the pH 6 by ammonia solution (NH_3 , 28-30%, SAMCHUN CHEMICAL). The adjusted mixture was stirred and heated to 85°C for 8 hr. An additional reflux system was applied to keep the concentration of

* INCHEON NATIONAL UNIVERSITY, DEPARTMENT OF MATERIALS SCIENCE & ENGINEERING, 119 ACADEMY-RO, YEONSU-GU, INCHEON, 22012, KOREA

Corresponding author: jjy309@inu.ac.kr

the mixture constant. The reacted sol was dried on a hot plate to make a gel. The completed gel was carried to a heat treatment in the atmosphere. The heat treatment conditions were 900-1300°C for 3-15 hours.

The crystal structure of U-type ferrite powder was analyzed by XRD (Rigaku, Cu K_{α} , $\lambda = 0.154$ nm, $2\theta = 20$ -80°). Grain size and morphology were observed by SEM (JEOL, JSM-7800F). In addition, saturation magnetization (M_s), coercivity (H_c), were measured by VSM (Quantum Design, VersaLab VSM, ± 10000 Oe, room temperature) to confirm the change of magnetic properties according to heat treatment conditions.

3. Results and discussion

Fig. 1 shows the X-ray diffraction patterns for the heat-treated samples. Fig. 1a-e show the samples with the heat treatment temperature increased from 900°C to 1300°C at 3 hours. And Fig. 1f-j show the samples with the heat treatment temperature increased from 900°C to 1300°C at 9 hours. It is shown the peaks corresponding to the U-type ferrite sintered conventional ceramic process [9-12] at the (e) heat treatment condition (1300°C for 3 hours). There are two major differences. First, there is a difference in time required for the formation of U-type ferrite. Except for the partially substituted Bi^{3+} U-type ferrite [12], the sintering condition in the solid state reaction process has 5-6 hours at 1250°C or higher [8-12]. This is a feature of the sol-gel method and generally sol-gel method has a relatively short time in the fabrication of the same material as compared to other fabricating methods [8,9]. The second is that, unlike the ceramic process, crystal growth is dominated by certain crystal plane. It is that Fig. 2 compares the X-ray diffraction patterns of the powder depending on the time at the same temperature. Fig. 2a-c show the X-ray diffraction patterns of specimens heat-treated at 1200°C for 3, 9 and 15 hours, respectively. And Fig. 2d-f show the X-ray diffraction

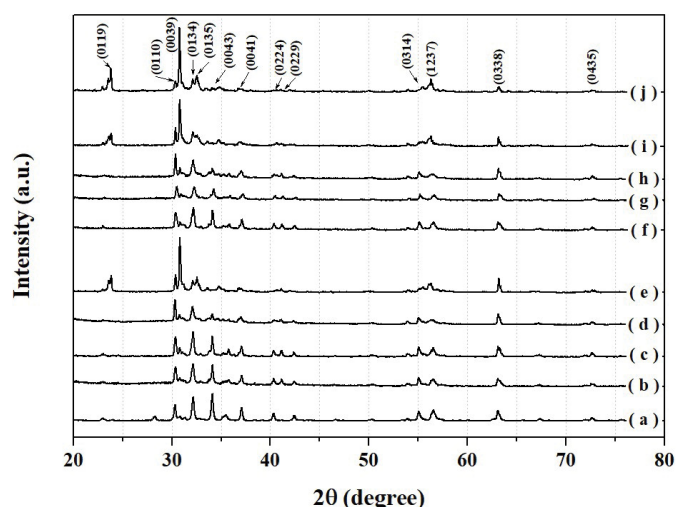


Fig. 1. XRD patterns for the different heat-treated samples; (a) 900, (b) 1000, (c) 1100, (d) 1200 and (e) 1300°C for 3 hr and (f) 900, (g) 1000, (h) 1100, (i) 1200 and (j) 1300°C for 9 hr

patterns of the specimens heat-treated at 1300°C for 3, 9 and 15 hours, respectively. The crystallization to (0039) plane has increased with an increase in the heat treatment time at both 1200°C and 1300°C. As a result, the plate-shaped grain has formed as shown in Fig. 3.

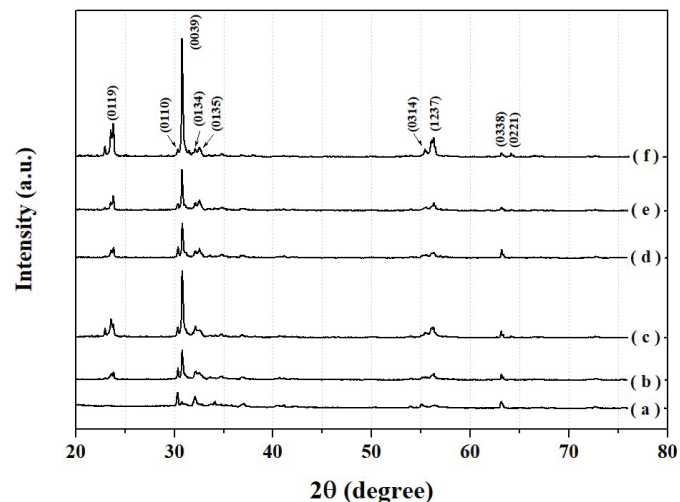


Fig. 2. XRD patterns for the different heat-treated samples; (a) 3, (b) 9 and (c) 15 hr at 1200°C and (d) 3, (e) 9, and (f) 15 hr at 1300°C

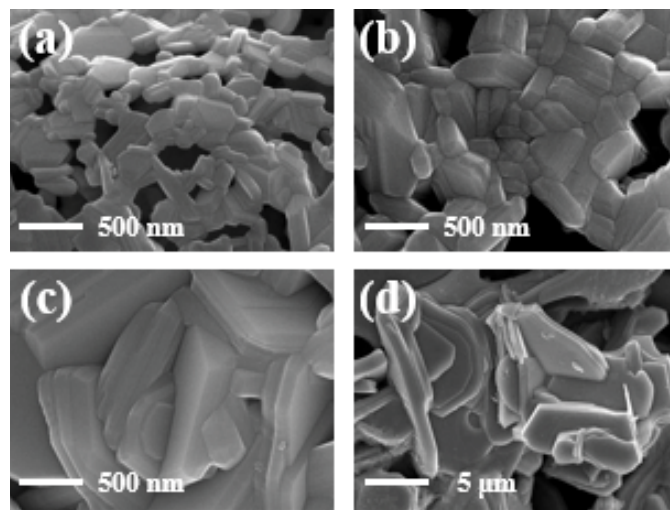


Fig. 3. SEM images of the heat-treated at different temperature for 3 hr; (a) 1000, (b) 1100, (c) 1200 and (d) 1300°C

Fig. 3 shows the SEM images of the powder heat-treated at different temperature for 3 hours. Fig. 3a,b show the samples heat-treated at 1000°C and 1100°C, respectively. As the heat treatment temperature increased, grains that several tens to several hundreds of nanometer have grown and connected to each other. In Fig. 3c, which corresponds to 1200°C, grain size has observed at sub- μm , and the morphology of grains starts to change from the granular-shape to the plate-shape. Fig. 3d shows that the sample was heat-treated at 1300°C. And it was observed to 5 μm or more connected plate-shaped grains. The tendency to exhibit such grain growth and plate-shaped grain formation was also observed in Fig. 4.

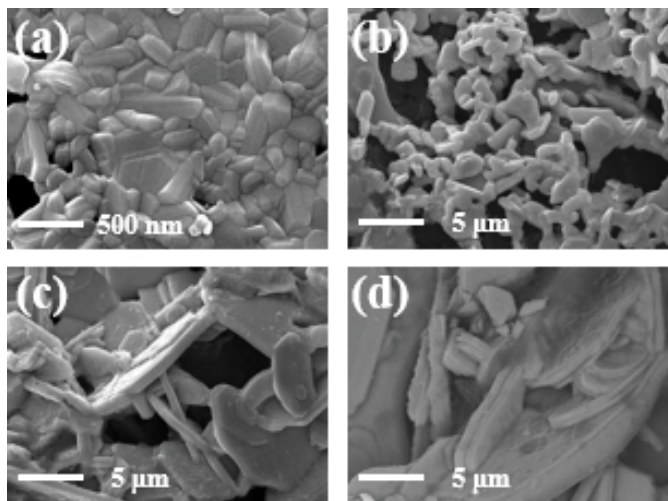


Fig. 4. SEM images of the heat-treated at different temperature for 9 hr; (a) 1000, (b) 1100, (c) 1200 and (d) 1300°C

Fig. 4 shows the SEM results of the powders heat-treated at different temperatures for 9 hours. Interestingly, Fig. 4a and Fig. 3b show similar results, and also in Fig. 4b and Fig. 3c observed grains have similar sub- μm size. Which it is previously referred to in the XRD analysis associated with U-type ferrite formation energy. Fig. 4c shows clear plate-shaped grains and Fig. 4d also shows an increase in the thickness of the plate-shaped grains. Fig. 5 has compared the changes in heat-treated samples for different times at 1300°C. Fig. 5a-c were heat-treated at 3, 9, and 15 hours, respectively. It was clearly confirmed that the gap between the plate-shaped grains disappeared with increasing the time. In the sample heat-treated for 15 hours, the plate-shaped grains were connected to each other in the vertical direction of the plate, and the shape was like contour lines. Which is consistent with the dominant growth of the grain on a particular crystal plane as shown in the XRD analysis.

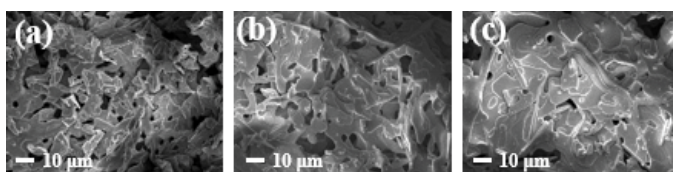


Fig. 5. SEM images of the heat-treated at different time at 1300°C; (a) 3, (b) 9, and (c) 15 hr

Fig. 6 and 7 show the magnetic properties (M-H curves) change of U-type ferrite according to the heat treatment time. Table 1 lists the saturation magnetization (M_s) and the coercivity (H_c) measured according to the heat treatment conditions. As shown in Figs. 6 and 7 and Table 1, as the heat treatment temperature increases, the M_s has increased and the H_c has decreased. The M_s has increased by ~ 5 emu/g at ~ 45 emu/g when the U-type ferrite began to form. On the other hand, the H_c shows a clear difference. As the U type ferrite began to form, the H_c has decreased to $\sim 1/3$. The increasing of the saturation magnetization, in other words, means stable U-type ferrite formation.

And decreasing of the coercivity has explained as a result of an increase in grain size. The inflection in Fig. 6 and Fig. 7 have interpreted to be caused by the phase transition. These inflection has disappeared from the heat treatment conditions where the U-type ferrite begins to form (1200°C in Fig. 6, 1100°C in Fig. 7). Fig. 8 shows the change of M_s and H_c with time at 1200°C and 1300°C. As shown in Fig. 8, the M_s was 50.0-54.0 emu/g that similar to the ceramic process (50-54 emu/g) [9-12]. The H_c was 529.0-177.7 Oe, which was higher than that of the ceramic process (14-127 Oe) [9-12]. The sample with high H_c (529.0 Oe) was subjected to the heat treatment condition at 1200°C for 3hr (Fig. 1d). As it can be seen from the XRD peak (Fig. 1d), the formation of U-type ferrite was not formed completely, therefore the H_c was high. Nevertheless, the H_c of the others were higher still than that of the ceramic process. These characteristics were caused by differences in the powder fabrication method. The ion location of sol-gel method has located more precisely in the crystal lattice than the ceramic process. Due to this difference,

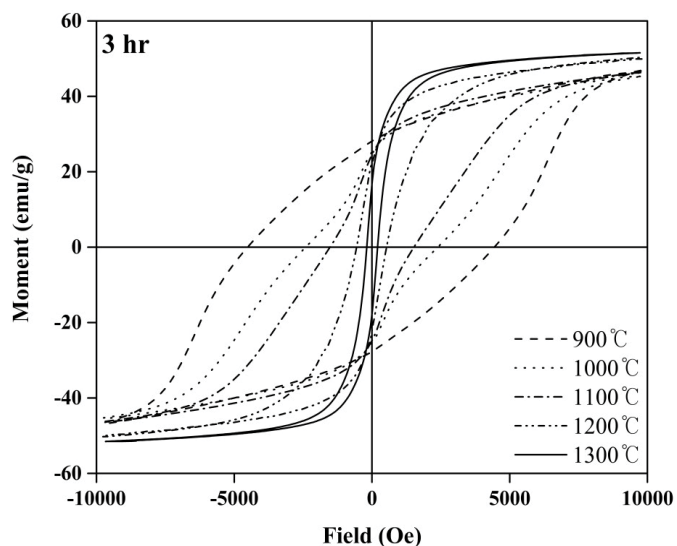


Fig. 6. M-H curves of the heat-treated at different temperature for 3 hr

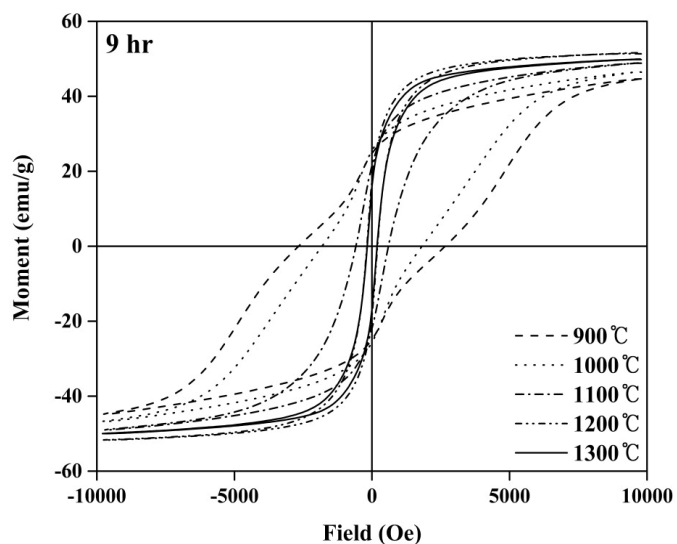
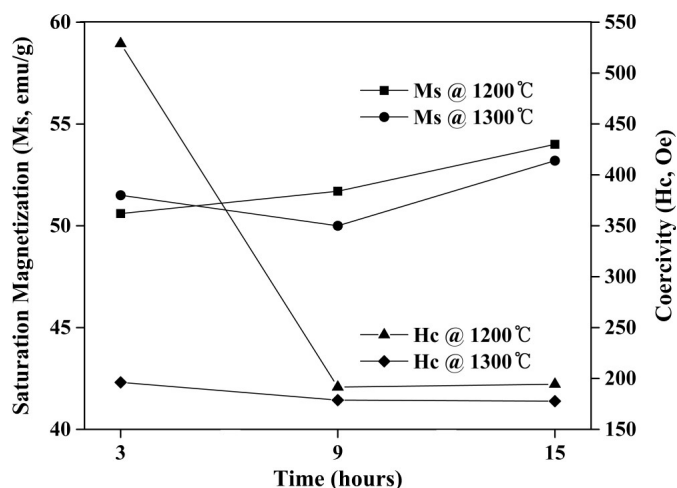


Fig. 7. M-H curves of the heat-treated at different temperature for 9 hr

Magnetic properties of U-type ferrite according to heat treatment conditions

Time (hr)	Temp. (°C)	M_s (emu/g)	H_c (Oe)	Time (hr)	Temp. (°C)	M_s (emu/g)	H_c (Oe)
3	900	46.8	4477.8	9	900	44.7	2664.6
	1000	45.4	2394.8		1000	46.7	1820.0
	1100	46.3	1522.8		1100	49.0	589.0
	1200	50.6	529.0		1200	51.7	191.5
	1300	51.5	196.2		1300	50.0	178.8
15	1200	54.0	194.4	15	1300	53.2	177.7

Fig. 8. Changes of saturation magnetization (M_s) and coercivity (H_c) at 1200°C and 1300°C

the magnetocrystalline anisotropy of the powder by the sol-gel method was enhanced. As a result of the enhanced magnetocrystalline anisotropy, it has high H_c [13,14].

4. Conclusions

The crystal structure of the nano-powder fabricated by the sol-gel method confirmed that the U-type ferrite was produced similarly to the solid state reaction process at a relatively short time. As the heat-treated temperature and time increased, the crystal growth dominated by a certain crystal plane, and thus a plate-shaped grain was obtained. The size of the grains was more than a few tens of micrometers. The magnetic properties of the U-type ferrite by the sol-gel method showed similar M_s as compared with the ceramic process. Although the H_c was somewhat high, it was confirmed that excellent soft magnetic characteristics were exhibited. As a result, it was confirmed that the sol-gel method can fabricate the U-type ferrite similar to that produced through the solid state reaction process. In the future research, we will analyze the absorption characteristics of

U-type ferrite by sol-gel method and the calorimetric analysis. In addition, we will study the change of properties according to substitution or addition elements based on the easy stoichiometric control which is one of the advantages of the sol-gel method.

Acknowledgments

This work was supported by Incheon National University (International Cooperative) Research Grant in 2017

REFERENCES

- [1] Ü. Özgür, Y. Alivov, H. Morkoç, J. Mater. Sci. **20**, 789 (2009).
- [2] R.C. Pullar, Prog. Mater. Sci. **57**, 1191 (2012).
- [3] S. Kumar, R.S. Meena, R. Chatterjee, J. Magn. Magn. Mater. **418**, 194 (2016).
- [4] R.S. Meena, S. Bhattacharya, R. Chatterjee, Mater. Sci. Eng. B **171**, 133 (2010).
- [5] M.C. Dimri, S.C. Kashyap, D.C. Dube, IEEE Trans. Magn. **42**, 3635 (2006).
- [6] M.C. Dimri, H. Khanduri, H. Kooskora, I. Heinmaa, E. Joon, R. Stern, J. Magn. Magn. Mater. **323**, 2210 (2011).
- [7] D. Lisjak, P. Macguinness, M. Drogenik, J. Mater. Res. **21**, 420 (2006).
- [8] R.C. Pullar, A.K. Bhattacharya, J. Mater. Sci. **36**, 4805 (2001).
- [9] D. Lisjak, D. Makovec, M. Drogenik, J. Mater. Res. **19**, 2462 (2004).
- [10] S.R. Shannigrahi, W.Q. Au, V. Suresh Kumar, L. Liu, Z.H. Yang, C. Cheng, C.K.I. Tan, R.V. Ramanujan, J. Magn. Magn. Mater. **325**, 63 (2013).
- [11] K. Kamishima, R. Tajima, K. Watanabe, K. Kakizaki, A. Fujimori, M. Sakai, K. Watanabe, H. Abe, J. Magn. Magn. Mater. **375**, 54 (2015).
- [12] S. Kumar, R. Chatterjee, J. Magn. Magn. Mater. (2017).
- [13] S. Yang, J.G. Kim, Arch. Metall. Mater. **62**, 2B, 1197 (2017).
- [14] S. Yang, K.P. Jeong, S.Y. Park, J.G. Kim, Arch. Metall. Mater. **62**, 2B, 1201 (2017).